

# Molecular Recognition and Chemistry in Restricted Reaction Spaces. Photophysics and Photoinduced Electron Transfer on the Surfaces of Micelles, Dendrimers, and DNA

NICHOLAS J. TURRO,\*<sup>†</sup> JACQUELINE K. BARTON,<sup>‡</sup> and DONALD A. TOMALIA<sup>§</sup>

Chemistry Department, Columbia University, New York, New York 10027, Division of Chemistry and Chemical Engineering, California Institute of Technology, Pasadena, California 91125, and Michigan Molecular Institute, Midland, Michigan 48674

Received June 6, 1991 (Revised Manuscript Received September 18, 1991)

## Reactions in Restricted Spaces

This Account is concerned with molecular recognition in bimolecular reactions<sup>1</sup> that occur in restricted spaces.<sup>2</sup> Bimolecular reactions of interest are *photoinduced electron transfers* for which the reactants are positively *electronically excited metal complexes* (Figure 1) and another positively charged gegenion, either a metal complex or methyl viologen (MV<sup>2+</sup>) that serves as an electron acceptor. The restricted reaction spaces are the interfacial regions of *anionically charged polyions such as micelles, starburst dendrimers, and DNA*.

*Molecular recognition*<sup>3</sup> is concerned with how specific sites on a molecular receptor are recognized by a binding substrate. Knowledge of the underlying principles of molecular recognition is useful in diverse activities such as the design of site- and conformation-specific reagents for biomolecules, the rational design of drugs and probes of polymer structure, the design of efficient catalytic systems, the design of strategies leading to the synthesis of new materials, and the design of novel nanoscopic devices.

## Topological, Geometric, Chemical, and Dynamic Issues

For the purposes of this Account, a restricted space is an environment (the "receptor" structure) whose geometric features, in addition to its chemical features, control the chemical reactivity of a bound species (the "substrate" structure) by controlling the dynamics of transport, the details and orientations of collisions, and consequently, the efficiency and rate of the reaction.

Nicholas J. Turro was born in Middletown, CT, attended Wesleyan University (A.B., 1960), and was an NSF Predoctoral Fellow with George S. Hammond at Caltech (Ph.D., 1963). After an NSF postdoctoral fellowship with Paul D. Bartlett at Harvard, he joined the Columbia University Chemistry Department, where he is now the Wm. P. Schweitzer Professor of Chemistry. His research interests include photochemical probes of interfaces, reactions in constrained environments, magnetic effects on reactions, and molecular recognition in photochemical reactions.

Jacqueline K. Barton was born in New York City, attended Barnard College (B.A., 1974), and was an NSF Predoctoral Fellow with Stephen J. Lippard at Columbia (Ph.D., 1979). After postdoctoral work at Bell Laboratories and at Yale University as a NIH Fellow with R. G. Shulman, she joined the Chemistry Department at Hunter College. In 1983 she returned to Columbia University, where she was Professor of Chemistry and of Biological Sciences before joining the faculty in the Division of Chemistry & Chemical Engineering at Caltech. She was named a MacArthur Foundation Fellow in 1991.

Donald A. Tomalia was born in Owosso, MI, in 1938, attended the University of Michigan (Flint College; B.A., 1961), and joined the Dow Chemical Company as a research chemist in 1962. He progressed to the level of research manager while earning a Ph.D. from Michigan State University in physical-organic chemistry in 1968. Currently he holds the position of Research Professor at the Michigan Molecular Institute. He has received three national industrial research awards (IR-100 awards) for creative research and holds 83 U.S. patents. His main research interests include starburst dendrimers, molecular recognition, enzyme inhibition, molecular self-organization, controlled delivery systems, and precision design of macromolecules.

At the *topological level*,<sup>4</sup> the simplest topological space suitable for representation of a restricted reaction space is probably a simply connected closed space in three dimensions. Many chemically distinct restricted spaces are identical at the topological level, and therefore, although these spaces "all look different" as a structure in three-dimensional Euclidean space, they will share all fundamental topological features of the topological space, i.e., they "all look identical" to a topologist. Indeed, at the level of topology, aqueous solutions of many microheterogeneous systems (e.g., micelles, dendrimers, DNA) correspond to the same topological form as a simply connected closed space in three dimensions. At the *geometric level* of representation, an important issue is the ability to describe restricted spaces in a fundamental manner which gives the space a metric (length scales and angles), but for which chemical and energetic features are suppressed and only the global Euclidean features (idealized geometric objects) of the space are emphasized.

At the *chemical level*, we must consider the size of the restricted space as a global object, and the size of the sites which are accessible to binding of molecular probes. We must also consider such chemical details as the energetics (thermodynamics) which describe the characteristics of the binding of the substrate to the sites of a particular restricted reaction space.

At the *chemical dynamics level* of representation, we are concerned with issues of the rates of translational and rotational mobility of the substrates among the accessible sites of the receptor, the rates of interconversion of the receptor sites, the characteristic rates of the probe relaxations (physical and chemical), and the interplay of these dynamic features.

## Restricted Reaction Spaces with Charged Surfaces. Molecular Recognition

The top portion of Figure 2 shows schematically the "chemical" structures of an aqueous solution containing noncovalently bound, self-assembling polyion micellar aggregates<sup>5</sup> composed of an ionic surfactant possessing

<sup>†</sup> Columbia University.

<sup>‡</sup> California Institute of Technology.

<sup>§</sup> Michigan Molecular Institute.

(1) Benson, S. W. *Foundations of Chemical Kinetics*; McGraw-Hill: New York, 1960.

(2) (a) Drake, J. M.; Klafter, J.; Levitz, P. *Science* **1991**, *251*, 1574-1579. (b) Kalyanasundaram, K. *Photochemistry in Microheterogeneous Systems*; Academic Press, 1987. (c) Thomas, J. K. *The Chemistry of Excitation at Interfaces*; ACS Monograph; American Chemical Society: Washington, DC, 1984. (d) Gratzel, M. *Heterogeneous Electron Transfer*; CRC Press: Boca Raton, FL, 1989. (e) Klafter, J.; Drake, J. M. *Molecular Dynamics in Restricted Geometries*; Wiley: New York, 1989.

(3) Lehn, J. M. *Angew. Chem., Int. Ed. Engl.* **1988**, *27*, 90-112 and references therein.

(4) Turro, N. J. *Angew. Chem., Int. Ed. Engl.* **1986**, *25*, 882.

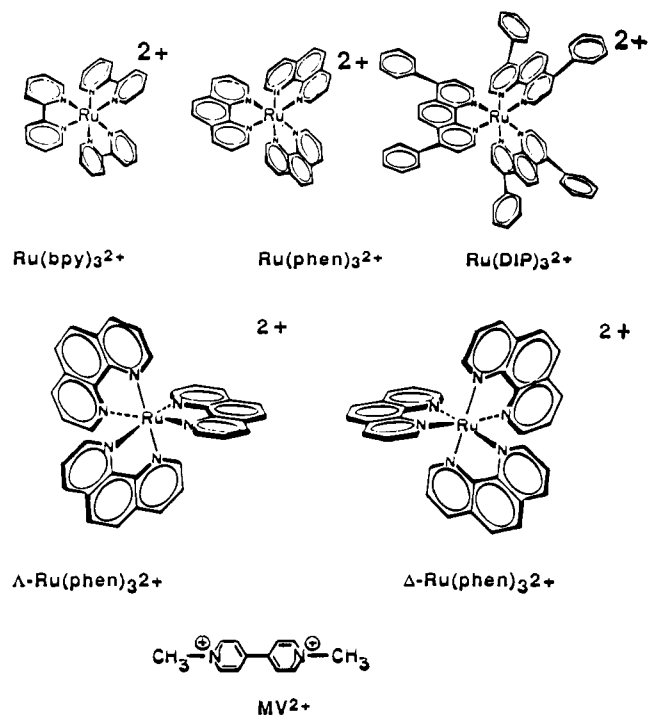


**Figure 1.** Ru complexes and electron-transfer quenchers discussed in this Account.

an anionic head group (the cationic gegenions required for charge compensation are not shown). The micellar aggregates are represented geometrically as a roughly spherical structure (left) and as a roughly cylindrical structure (right); which representation best describes a particular micellar aggregate depends on the experimental conditions (concentration of surfactant, ionic strength, temperature, etc.).<sup>6</sup> Also shown schematically in Figure 2 is a covalently connected starburst dendrimer polyion<sup>7</sup> possessing anionic carboxylate terminal groups, which is represented as having a spherical (or globular) shape, and a portion of covalently connected DNA polyion,<sup>8</sup> which is shown having a cylindrical (or rodlike) shape. The differing chemical appearances of these restricted spaces disguise the fact that at the level of topological geometry these structures are all identical to a simply connected space in three dimensions, i.e., each space has an outside (the bulk aqueous phase), a boundary (the charged interface between the bulk aqueous phase and the restricted space), and an inside (the hydrophobic core of the micelle, the hydrophilic core of the dendrimer, and the stacked base pairs of DNA). Thus, all aspects of molecular recognition involving any of these reaction spaces will share these common topological features.

### A Simple Model of an Electrically Charged Liquid-Liquid Interface

Figure 3 describes schematically, but quite generally, the space in the vicinity of a negatively charged interface, based on the classical "double layer" model of a

charged electrode,<sup>9</sup> i.e., the anionically charged surface interfacing with the aqueous solution and possessing a distribution of positively charged counterions trapped by Coulombic forces in the vicinity of the interface.<sup>10</sup> In aqueous solutions, the electrical double layer<sup>9</sup> of a liquid-liquid interface is viewed as consisting of two regions: (a) a "compact" layer of ions at the interface of the charged surface and the aqueous phase, termed the Stern layer (typical size ca. 5–10 Å for simple, singly charged head groups and counterions); and (b) a "diffuse" layer extending beyond the interface surface, termed the Gouy-Chapman layer (extending tens to hundreds of angstroms normal to the surface of the interface).

The "fraction of gegenions bound" to the Stern layer will depend on conditions, but is typically<sup>11</sup> on the order of 50–75% (depending on factors such as the valency of the head groups and the counterions). Although mobile within the Gouy-Chapman layer, the "territorially bound" gegenions are "trapped" by the powerful electrostatic field generated by the Stern layer and are dynamically constrained in their diffusional transport to the "shell" or the "collar" about the interface representing the Gouy-Chapman layer. Finally, for the systems of greatest interest to this Account, i.e., starburst dendrimers and DNAs, there exists an organic phase or inner core, consisting of the fractally radiating arms of the dendrimer and the base pairs of the DNA, respectively.

### Binding Sites on Anionically Charged Polyions. Molecular Recognition

Figure 3 allows us to define the terms for the general types of binding sites for ruthenium (Ru) complexes of Figure 1 to any anionic polyion. Site I (far left) refers to the "unbound" complex in the bulk aqueous phase; site II refers to the *territorially bound* complex in the Gouy-Chapman layer; site III refers to the *ionic-site-bound* complex associated with a single charged head group in the Stern layer; site IV refers to the *surface-bound* complex associated with cooperative binding, such as that which might arise from attraction to a cluster of head groups or to a combination of ionic and hydrophobic interactions; and site V refers to the *intercalatively bound* complex associated with specific hydrophobic or structural interactions with the internal core.

These terms allow a concise and intuitive expression of much of the experimental data pertinent to the photophysics and photochemistry of metal complexes bound to anionic polyions. Of the five sites, we expect only a negligible fraction of the metal complex gegenions to be in the bulk aqueous phase, so that we shall seek to interpret our results only in terms of binding to sites II, III, IV, and V. Intuitively, territorial (site II) and/or ionic (site III) binding are not expected to possess sensitivity to the size, shape, or chirality of the Ru complex gegenions (no molecular recognition).

(5) (a) Fendler, J. H. *Membrane Mimetic Chemistry*; John Wiley: New York, 1982. (b) Fendler, E. J.; Fendler, J. H. *Catalysis in Micellar and Macromolecular Chemistry*; Academic Press: New York, 1975.

(6) (a) Rosen, M. J. *Surfactant and Interfacial Phenomena*, 2nd ed.; Wiley: New York, 1989. (b) Hiemenz, P. C. *Principles of Colloid and Surface Chemistry*, 2nd ed.; Dekker: New York, 1986.

(7) Tomalia, D. A.; Naylor, A. M.; Goddard, W. A., III. *Angew. Chem., Int. Ed. Engl.* 1990, 29, 138 and references therein.

(8) Saenger, W. *Principles of Nucleic Acid Structure*; Springer-Verlag: New York, 1984.

(9) Adamson, A. W. *Physical Chemistry of Surfaces*; Wiley-Interscience: New York, 1990; Chapter 5, p 203 ff.

(10) (a) Manning, G. S. *Q. Rev. Biophys.* 1978, 2, 179–246. (b) Friedman, R. A. G.; Manning, G. S.; Shahin, M. A. In *Chemistry and Physics of DNA-Ligand Interactions*; Kallenbach, N. R., Ed.; Adenine Press: New York, 1988; pp 36–64. (c) Manning, G. S. *Biophys. Chem.* 1977, 7, 95–102. (d) Manning, G. S. *Acc. Chem. Res.* 1979, 12, 443–449.

(11) Morawetz, H. *Macromolecules in Solution*, 2nd ed.; Wiley: New York, 1975. Manning, G. S. *Biophys. Chem.* 1977, 7, 95–102.

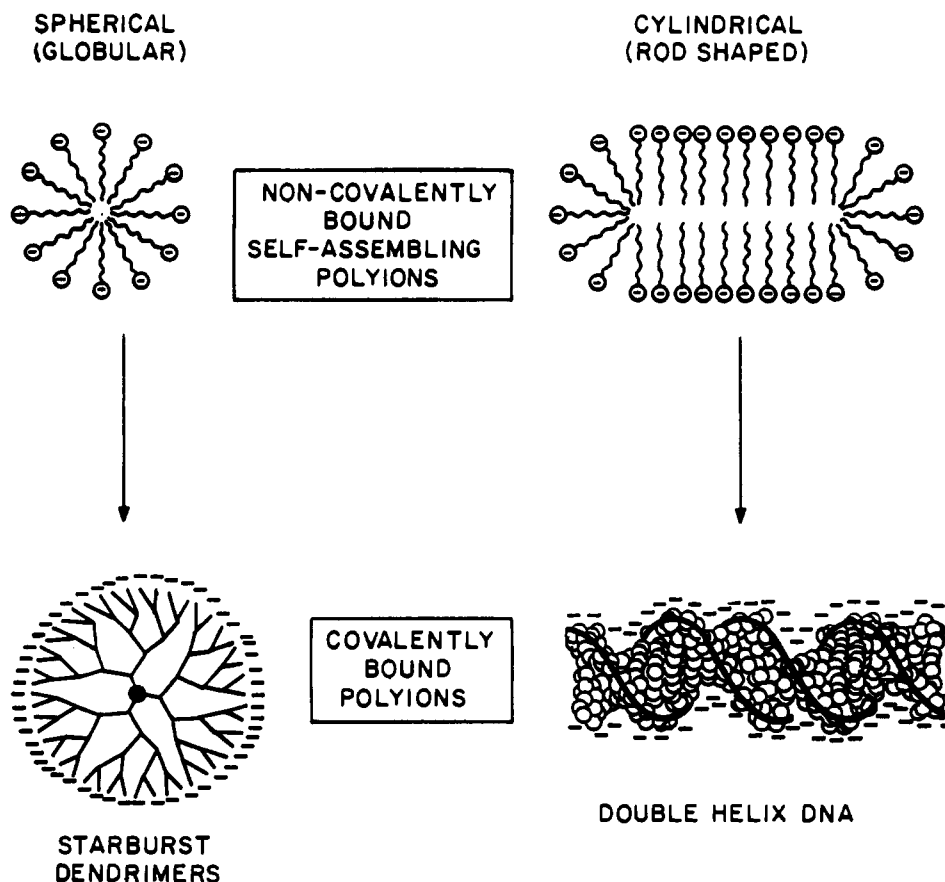


Figure 2. Schematic structures of micelles, dendrimers, and DNA. See text for discussion.

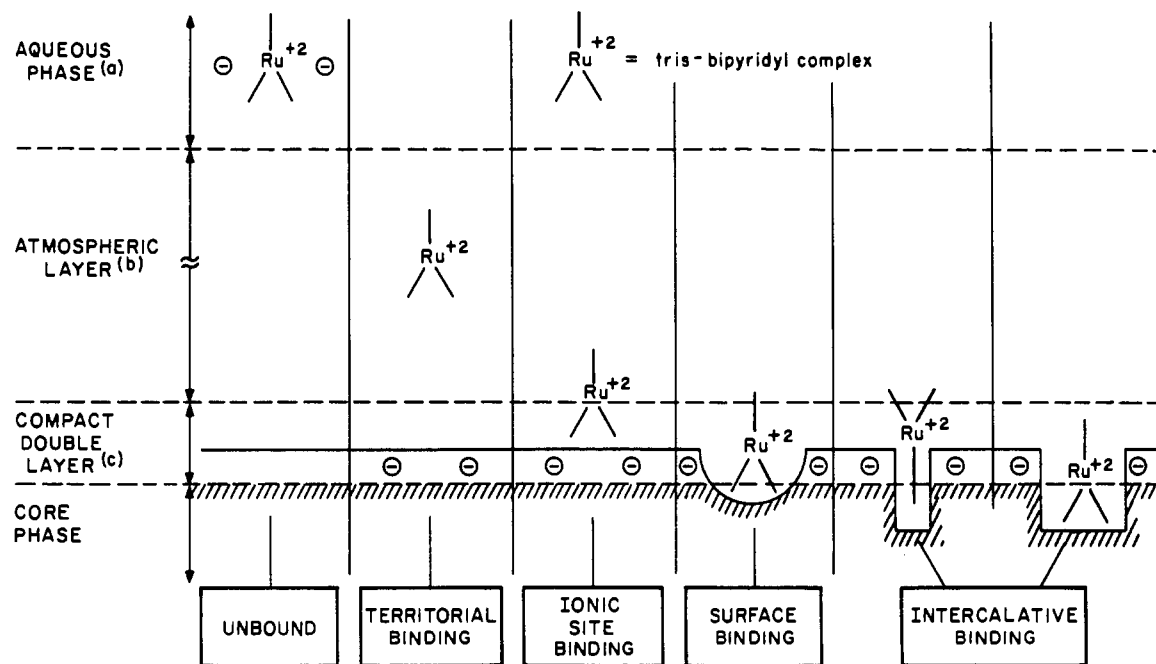


Figure 3. Sites for binding of metal complexes near an anionic interface: (a) Debye-Hückel region; (b) Gouy-Chapman region; (c) Stern region.

Surface (site IV) and intercalative (site V) binding will be sensitive to the size, shape, and chirality of the Ru complexes (molecular recognition possible). Finally, molecular recognition in terms of chiral discrimination and selectivity should be greater for intercalative binding than for surface binding because of the more intimate substrate-receptor structural contacts required for the intercalative mode.

### Photophysics of $\text{RuL}_3$ Complexes

The photophysical properties of  $\text{RuL}_3$  complexes make them attractive as photophysical probes for examining binding to polyions<sup>12</sup> and as models for solar energy storage:<sup>13</sup> an intense absorption in the visible

(12) Meyer, T. J. *Pure Appl. Chem.* 1990, 62, 1003-1009.

(13) Fox, M. A., Chanon, M., Eds. *Photoinduced Electron Transfer*; Elsevier: Amsterdam, 1988; Vol. 2.

region of the spectrum ( $\lambda_{\max}^{\text{H}_2\text{O}} \sim 452 \text{ nm}$ ,  $\epsilon_{\max}^{\text{H}_2\text{O}} \sim 15\,000 \text{ M}^{-1} \text{ cm}^{-1}$ ); a relatively intense and readily detectable emission in the visible region ( $\lambda_{\max}^{\text{H}_2\text{O}} \sim 610 \text{ nm}$ ,  $\Phi^{\text{H}_2\text{O}} \sim 0.04$ ); and a relatively long emission lifetime ( $\tau^{\text{H}_2\text{O}} \sim 500\text{--}1000 \text{ ns}$ ). Both the absorption and emission arise from a localized metal to ligand charge transfer transition (MLCT). Absorption is to a singlet state  $S_1(\text{MLCT})$ , and the origin of the emission is a (strongly mixed) nominal triplet state,  $T_1(\text{MLCT})$ , achieved after intersystem crossing from  $S_1(\text{MLCT})$ . The electronic structure of a MLCT state may be described as  $\text{Ru}^{\text{III}}(\text{bpy})_2(\text{bpy}^-)^{2+}$ , i.e., the metal center has been oxidized and a ligand has been reduced. Thus, the perimeter of the excited complex tends to be electron rich and a good reducing agent.

Because  $^*\text{Ru}(\text{bpy})_3^{2+}$  has a reduced ligand on the periphery of the complex, and because it is the reduced ligand and not the metal that interacts strongly with the environment of the complex, it is not surprising that the properties of a MLCT state are sensitive to the properties of the environment, if bound interfacially. In general, upon binding to an anionic interface, it is found that both the emission intensity ( $I$ ) and emission lifetime ( $\tau$ ) increase significantly.<sup>14</sup> There is a firm theoretical basis for the effect: binding to anionic interfaces increases the energy gap between  $T_1(\text{MLCT})$  and a thermally accessible metal-centered (MC) state that undergoes rapid radiationless deactivation. A larger gap is produced upon binding to an anionic interface, and this reduces the thermal population of the (nonradiative) MC state, which causes increases in  $I$  and  $\tau$  of  $T_1(\text{MLCT})$ .

In summary, simple photophysical parameters of steady state emission intensity ( $I$ ) and lifetime ( $\tau$ ) of  $\text{RuL}_3$  probes provide valuable clues as to the extent and the nature of binding (territorial, site, surface, or intercalative) of metal complexes to anionic polyions.

### Photophysical Parameters for Binding to Anionic Polyions

When  $^*\text{RuL}_3$  association with an anionic polyion involves hydrophobic interactions,<sup>14</sup> competing radiationless processes are inhibited so that binding leads to an increase in  $I$  relative to that observed in the aqueous phase. Thus, a simple qualitative guide to binding of  $\text{RuL}_3$  complexes to an anionic polyion is the magnitude of  $I$  and  $\tau$  in the presence of the polyion relative to the value of  $I_0$  and  $\tau_0$  in the absence of the polyion.

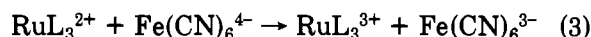
When the decay fits a single exponential, there is only one binding site, or if there is more than one binding site, multiple sites are equilibrating rapidly on the time scale of measurement (ca.  $(0.5\text{--}1) \times 10^{-6} \text{ s}$ ). If there are two (or more) sites from which emission occurs and the lifetime of emission at the sites differs substantially (ca. a factor of 2), fitting programs are available to fit the decay curve to values of  $\tau$  for each site, and for determining the fraction of population emitting from each site (vide infra). Thus, measurement of the parameter  $\tau$  provides information not only on whether the probe is strongly or weakly bound to the polyion but, in ad-

dition, on whether it is bound to more than one site and on the relative populations if two sites are revealed.

Further information on the mode of binding can be obtained from measurements of steady state emission polarization,  $\rho$ . If the metal complex is located at a site that does not restrict the motion of the probe, it will tumble freely and rapidly lose any initial polarization obtained by the absorption of polarized light. If, on the other hand, the metal complex is located at a site that restricts its motion, the magnitude of the polarization will be related to the extent of inhibition of motion, with an extreme of being immobilized (as in the solid phase), at which point a limiting maximum value of  $\rho$  will be obtained.

### Photochemical Aspects of $\text{RuL}_3$ Complexes. Photoinduced Electron Transfer

$\text{RuL}_3$  complexes also possess excellent photochemical characteristics for determining the rates of photoinduced electron transfer,<sup>13</sup> which can be converted to parameters to examine the dynamics of reactions and the mobility of the complexes adsorbed on or near anionic interfaces. These attractive photochemical properties of  $\text{Ru}(\text{bpy})_3^{2+}$  include the following: a strong driving force for electron transfer from  $^*\text{Ru}(\text{bpy})_3^{2+}$  to electron acceptors (and for electron transfer to  $\text{Ru}(\text{bpy})_3^{2+}$  from electron donors) and a bimolecular rate constant ( $k_{\text{et}}$ , units liters/(mole second)) for photoinduced electron transfer with many electron donors and acceptors that is close to that for diffusion ( $10^{10} \text{ M}^{-1} \text{ s}^{-1}$ ) in water. For example, photoinduced electron transfer to acceptors of the same charge ( $\text{MV}^{2+}$  or  $\text{CoL}_3^{3+}$ , eqs 1 and 2, respectively) occurs with  $k_{\text{et}} \sim 1 \times 10^9 \text{ M}^{-1} \text{ s}^{-1}$ , and photoelectron transfer to  $\text{Fe}(\text{CN})_6^{4-}$  as acceptor (eq 3) occurs with  $k_{\text{et}} \sim 1 \times 10^{10} \text{ M}^{-1} \text{ s}^{-1}$ .



### Structural Aspects of $\text{RuL}_3$ Complexes and Their Role in Molecular Recognition

One of the most important criteria for efficient molecular recognition is a high degree of complementarity of substrate structure and receptor structure in the bound complex. These criteria imply physical, noncovalent contact between substrate and receptor over an area that is commensurate with a significant portion of the substrate. Such contacts contain the information that allows the receptor to sense the structure of the substrate and achieve selectivity in binding. Since the ligands, and not the metal center of the  $\text{RuL}_3^{2+}$  complexes, come in contact with the receptor structure in the Stern layer of polyions, it is the size and shape of the ligand exterior and not the metal that will be dominant in determining the recognition features for a polyion receptor. Many tris(bipyridyl) complexes of Ru(II) possess structures that may be designed to be complementary to a highly selective receptor such as DNA.

### Starburst Dendrimers: Spherical Restricted Reaction Spaces

Starburst dendrimers are a novel class of macromolecules having a definite molecular composition and

(14) (a) Meisel, D.; Matheson, M. S.; Rabini, J. *J. Am. Chem. Soc.* 1978, 100, 117–122. (b) Hauenstein, B. L.; Dressick, W. J.; Buell, S. L.; Demas, J. N.; DeGraff, B. A. *J. Am. Chem. Soc.* 1983, 105, 4251–4255. (c) Dressick, W. J.; Hauenstein, B. L.; Demas, J. N.; DeGraff, B. A. *Inorg. Chem.* 1984, 23, 1107. (d) Dressick, W. J.; Cline, J.; Demas, J. N.; DeGraff, B. A. *J. Am. Chem. Soc.* 1986, 108, 7567–7574.

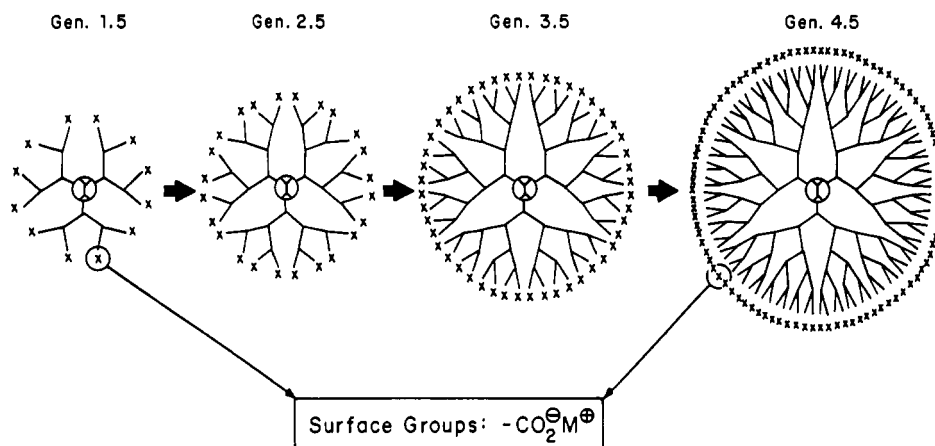


**Figure 4.** Schematic representation of starburst dendrimers. The central vertex is a nitrogen atom core. The repeat unit corresponding to the line in a branch is  $\text{CH}_2\text{CH}_2\text{CONHCH}_2\text{CH}_2\text{N}$ .

constitution.<sup>7</sup> The central vertex is a nitrogen core atom, and each radiating branch is a  $\text{CH}_2\text{CH}_2\text{CONHCH}_2\text{CH}_2\text{N}$  unit (Figure 4). The branches at the external surface of the macromolecules may be terminated at an ester stage, which is termed a half-generation,  $n.5$  G (if termination occurred at an amine stage, they are called full generation or  $n.0$  G dendrimers). Since the radial branches all involve covalent bonding, starburst dendrimers possess a well-defined composition and constitution, but their shapes, morphologies, and in particular, their surface properties have not yet been directly characterized by spectroscopic techniques.

Molecular simulations<sup>15</sup> provide evidence that the morphology, and therefore the surface characteristics, of the dendrimers change dramatically as the size of the dendrimer increases. For example, the simulations show that while "earlier" generations (1–3 G) possess a highly asymmetric, open, "starfish-like" shape, the "later" generations ( $>4$  G) possess a nearly spherical shape. Also, the average structures of the earlier generations ( $<3$  G) are very open, whereas the later generations ( $>4$  G) are more closed, densely packed structures.

The carboxylate sodium salts of the half generation ( $n.5$  G,  $n = 0-9$ ) poly(amidoamine) or PAMAM dendrimers, derived from hydrolysis of the terminal ester groups, represent a new class of anionic polyions. It was of interest to determine whether photoinduced electron transfer could serve as a probe of the morphological changes predicted to occur as a function of increasing dendrimer size.

### Photophysics of $\text{RuL}_3$ Complexes in the Presence of Starburst Dendrimers

Evidence for a qualitative difference in the binding of  $\text{RuL}_3$  complexes to the "earlier" and "later" generations was found in the measurement of the photophysical parameters  $I$  and  $\tau$ . The "earlier" generations were experimentally defined as 0.5–2.5 G from the observations that both  $I$  and  $\tau$  were indistinguishable in the presence or absence of these dendrimers up to concentrations<sup>16</sup> of ca. 10 mM head groups (corresponding to a large excess of the anionic sites). In contrast, the

values of  $I$  and  $\tau$  were strongly enhanced for the "later" generations, 3.5–9.5 G. Furthermore, the luminescence decay in the presence of the "later" generations was a single exponential, consistent with a single site (or time-averaged multiple sites) for binding on the dendrimer surface. Finally, NMR evidence suggested that the  $\text{RuL}_3$  complexes were bound to the dendrimer surface and not to the dendrimer core. In terms of the sites of Figure 3, we consider the complexes to be best classified as *site bound to the Stern layer* for the later generations and *unbound or in the Gouy–Chapman layer* for the earlier generations.

### Photoinduced Electron Transfer in the Presence of Anionic Starburst Dendrimers

We first investigated the photoinduced electron transfer from  $\text{RuL}_3$  complexes to gegenion acceptors adsorbed on anionic micelles derived from sodium alkyl sulfates<sup>17,18</sup> because these micelles provide a simple restricted space and detailed kinetic equations for analysis of the dynamics of excited-state quenching have been established and tested for various limiting cases.<sup>16</sup> These analyses provide, under favorable conditions, extraction of the bimolecular rate constant for electron transfer ( $k_{\text{et}}$ ) between the excited complex and a quencher, under conditions such that the rate of exit of the probe and the quencher from a micelle is slow relative to intramolecular quenching on the micelle. In this manner, values of  $k_{\text{et}}$  were successfully extracted from the data for anionic micelles.<sup>17,18</sup>

The quenching of MLCT luminescence of  $\text{Ru}(\text{phen})_3^{2+}$  by electron transfer to  $\text{MV}^{2+}$  as electron acceptor was investigated in the presence and absence of dendrimers of various sizes (0.5–9.5 G), and the results were compared to those for photoinduced electron transfer in aqueous solutions (Table I). In the presence of "earlier" generations (0.5, 1.5, and 2.5 G), the quenching of  $^*\text{Ru}(\text{phen})_3^{2+}$  luminescence *did not follow the analysis for micellar systems*, but instead followed the normal Stern–Volmer bimolecular kinetics expected for bimolecular quenching in homogeneous solution. The values of  $k_{\text{et}}$  for each of the earlier generations were ca.  $5.0 \times 10^9 \text{ M}^{-1} \text{ s}^{-1}$  (a bimolecular reaction) and are

(15) Naylor, A. M.; Goddard, W. A., III; Kiefer, G. E.; Tomalia, D. A. *J. Am. Chem. Soc.* 1989, 111, 2341.

(16) (a) Moreno-Bondi, M.; Orellana, G.; Turro, N. J.; Tomalia, D. A. *Macromolecules* 1990, 23, 910. (b) Caminati, G.; Turro, N. J.; Tomalia, D. A. *J. Am. Chem. Soc.* 1990, 112, 8515.

(17) (a) Miyashite, T.; Murakata, T.; Matsuda, M. *J. Phys. Chem.* 1983, 87, 4529. (b) Miyashite, T.; Murakata, T.; Yamaguchi, Y.; Matsuda, M. *J. Chem. Phys.* 1985, 89, 497–500.

(18) Gopidas, K. R.; Leheny, A. R.; Caminati, G.; Turro, N. J.; Tomalia, D. A. *J. Am. Chem. Soc.*, in press.

**Table I.**  
**Quenching Rate Constants for Luminescence Quenching of**  
**Ru(phen)<sub>3</sub><sup>2+</sup> by MV<sup>2+</sup> in Various Starburst Dendrimers**

starburst	$k_q^a$	$R, \text{Å}^b$
control <sup>c</sup>	$5.0 \times 10^9 \text{ M}^{-1} \text{ s}^{-1}$	
0.5 G	$5.6 \times 10^9 \text{ M}^{-1} \text{ s}^{-1}$	14
1.5 G	$4.1 \times 10^9 \text{ M}^{-1} \text{ s}^{-1}$	18
2.5 G	$4.9 \times 10^9 \text{ M}^{-1} \text{ s}^{-1}$	24
3.5 G	$1.2 \pm 0.6 \times 10^7 \text{ s}^{-1}$	33
4.5 G	$7.4 \pm 0.5 \times 10^6 \text{ s}^{-1}$	44
5.5 G	$5.1 \pm 0.4 \times 10^6 \text{ s}^{-1}$	56
6.5 G	$2.3 \pm 0.3 \times 10^6 \text{ s}^{-1}$	63
7.5 G	$1.8 \pm 0.3 \times 10^6 \text{ s}^{-1}$	74
8.5 G	$7.7 \pm 0.4 \times 10^5 \text{ s}^{-1}$	87
9.5 G	$6.4 \pm 0.4 \times 10^5 \text{ s}^{-1}$	105

<sup>a</sup> Rate constants for photoinduced electron transfer. For the 1.5 G and 2.5 G, the rate constants are bimolecular and experimentally indistinguishable from the rate in water in the absence of dendrimer. The [Ru(phen)<sub>3</sub><sup>2+</sup>] to [SBD] ratio was  $\leq 0.1$  in all cases. Error limits: approximately 10% of the reported values. <sup>b</sup> Radius of the indicated dendrimer (Å) determined by size-exclusion chromatography. See: Caminati, G.; Turro, N. J.; Tomalia, D. A. *J. Am. Chem. Soc.* 1990, 112, 8515. <sup>c</sup> Bimolecular rate constant for electron transfer from \*Ru(phen)<sub>3</sub><sup>2+</sup> to MV<sup>2+</sup> in aqueous solution, adjusted for typical ionic strength of the dendrimer solutions.

experimentally indistinguishable from the values found for aqueous solutions in the absence of dendrimers. However, in the presence of the "later" generations (3.5–9.5 G), the data followed the micellar analysis to a high degree of accuracy, suggesting a change of mechanism for the electron-transfer process. The values of  $k_{et}$  decreased systematically from ca.  $1.2 \times 10^7 \text{ s}^{-1}$  for 3.5 G to ca.  $6.4 \times 10^5 \text{ s}^{-1}$  for 9.5 G (note that the units are for a unimolecular reaction).

Evidently, the earlier generations possess an open structure and charged surface and behave as simple electrolyte anions, not as polyions or restricted reaction spaces. However, the later generations (3.5–9.5 G) possess closed Stern layer surface structures and behave as anionically charged (time averaged) spherical restricted reaction spaces. The "closing" of the surface creates information that provides molecular recognition capable of binding and organizing the reactants into a nanoscopic restricted reaction space, at the anionically charged dendrimer surface. Further support for binding to the Stern layer was derived from the strong inhibition of quenching of MLCT luminescence of Ru(phen)<sub>3</sub><sup>2+</sup> by electron transfer to the negatively charged electron transfer quencher Fe(CN)<sub>6</sub><sup>4-</sup>, which is effectively repelled from the dendrimer surface in the presence of the later, but not the earlier, generations.

These conclusions are consistent with the predicted "open" structure of the earlier generations and the "closed" surface structure of the later generations predicted by molecular mechanics simulations.<sup>15</sup> When both gegenions are bound to the Stern layer of a single later generation dendrimer molecule, electron transfer is "unimolecular" in the sense that it occurs during the lifetime of the complex on the surface of a single dendrimer particle. As the ends of a flexible polymethylene biradical are "connected" unimolecularly by a chain of CH<sub>2</sub> groups, the Ru(phen)<sub>3</sub><sup>2+</sup> and MV<sup>2+</sup> are "connected" by binding to the surface of a dendrimer molecule. This binding leads to a great specificity in the electron-transfer step: only acceptors "bound" to the Ru(phen)<sub>3</sub><sup>2+</sup> through the dendrimer surface are effective as quenchers. An interesting aspect of the quantitative results is the decrease of the rate constants,  $k_{et}$ , as the

dendrimer size increases for 3.5–9.5 G (33–105-Å radius). Whether this systematic decrease is the result of the systematic increase in the dendrimer surface area (a geometric effect) or is the result of an increased "friction" toward diffusional motion is an issue currently under investigation.

### DNA as a Restricted Reaction Space

Under physiological conditions, DNA is an anionic polyion composed of the famous heterocyclic bases (A, C, T, G) connected together through a linear polymeric sugar phosphate backbone.<sup>8</sup> The ionized phosphate groups are the anionic charges of the polyion surface. In the double-stranded forms, the two DNA polyanions are associated noncovalently, stabilized by the H-bonding and  $\pi$ -stacking interactions of the bases, and the polymer forms a double-helical structure with two negative charges/base-pair unit. In contrast to the spherical later generation dendrimers, DNA is better modeled as a very long, thin, double-stranded cylinder. Thus, a double-stranded DNA molecule, as a restricted reaction space, may be described geometrically as possessing an idealized cylindrical shape whose hydrophobic interior is the base-pair core and whose hydrophilic surface corresponds to the electrical double layer (the Stern layer). This layer, in turn, is surrounded by a very polar and hydrophilic cylindrical "collar" which corresponds to the ionic atmosphere of gegenions (the Gouy-Chapman layer). The characteristic radius of the core cylinder is generally constrained to a small range (ca. 20–25 Å and defined by the size of the base pairs), but the characteristic length of the cylinder may be very considerable (from tens of angstroms for synthetic oligonucleotides and tens of thousands of angstroms for naturally occurring DNA).

Geometrically, DNA exists in several important conformations that introduce different textures to the double-layer surface exposed to the aqueous phase.<sup>19</sup> Of these conformations, we shall consider mainly the so-called B form in this Account. The B form of DNA exists<sup>8</sup> as a right-handed spiraling double helix consisting of base pairs stacked in the center of the double helix with the average base plane being normal to the helical (cylindrical) axis. This conformation possesses two well-defined "grooves", termed the "major" groove (depth ca. 25 Å into the surface of the double helix) and the "minor" groove (depth ca. 10 Å into the surface of the double helix), which texture the double-helical strand with characteristic shapes. The binding of the Ru complexes to DNA is thus a sensitive function of the size, shape, and hydrophobic characteristics of the complex as determined by the chemical structure of the ligands of the complex. From the standpoint of molecular recognition,<sup>20</sup> a high degree of sensitivity to substrate structure is expected to be achieved with DNA, when a portion of the substrate structure is accessible to and has a size commensurate with the minor grooves or major grooves. Furthermore, the helical shape of DNA makes these grooves chiral and therefore capable of recognizing one substrate enantiomer from another.<sup>21</sup> In effect, with respect to binding sites, the DNA surface is "rough" geometrically (sensitive to the

(19) Barton, J. K. *Science* 1986, 233, 727–734.

(20) Thurston, D. E.; Thompson, A. S. *Chem. Br.* 1990, 767–772.

(21) Barton, J. K. *Comments Inorg. Chem.* 1985, 3, 321.

shape of the receptor) and "heterogeneous" chemically (different interaction energies at the different binding sites).

Chemically, the internal "core" phase of the cylinder is composed of the famous hydrogen-bonded base pairs and the double layer consists of the surface fixed anionic phosphate head groups and gegenions in the Stern and Gouy–Chapman layers. Simple monovalent metal gegenions such as sodium in the Gouy–Chapman layer are expected to be very mobile compared to the gegenion in the Stern layer. The same mobility in the Gouy–Chapman layer is expected for complex "outside" counterions such as the Ru complexes; however, because of size, shape, and symmetry effects, because of possible "hydrophobic" interactions, and because of the special intercalative interactions, the mobility of the "inside" Ru complexes bound in the Stern layer may be considerably decreased.

### Photophysical Measurements of Binding Modes of Metal Complexes to DNA

The emission intensity,  $I$ , and the lifetime,  $\tau$ , of  $^*Ru(bpy)_3^{2+}$  undergo no measurable change in the presence of B-DNA, indicating feeble binding to the DNA interface, or rapid equilibration of a bound species with the territorial site.<sup>22</sup> Furthermore,  $\tau$  for  $^*Ru(bpy)_3^{2+}$  is strictly a single exponential in the absence or presence of (a several-molar excess of) DNA. Finally, the value of  $\rho$  is identical to the value in water (ca. 0.0) even in the presence of (a large molar excess of) DNA. From our working model of a polyion, we tentatively conclude that the  $^*Ru(bpy)_3^{2+}$  is territorially bound to the interfacial region of the restricted space or, if it is bound to the DNA, it is in rapid equilibrium with the territorial phase.

In contrast to the results for  $Ru(bpy)_3^{2+}$ , all three photophysical parameters suggest that  $Ru(phen)_3^{2+}$  and  $Ru(DIP)_3^{2+}$  are both more tightly bound to DNA. First, there is a significant increase (ca. 300%) in the  $I$  of both complexes in the presence of DNA relative to the  $I$  in the absence of DNA. Next, there is a significant polarization observed for both complexes in the presence of DNA. Both  $Ru(phen)_3^{2+}$  and  $Ru(DIP)_3^{2+}$  show strictly single exponential emission decay in the absence of DNA. In the presence of DNA, the decay is fit by a biexponential function (eq 4) for both complexes.<sup>22,23</sup> In eq 4,  $A_f$  stands for the amplitude or fraction of the faster decaying population with lifetime  $\tau_f$ , and  $A_s$  stands for the amplitude or fraction of the slower decaying population with lifetime  $\tau_s$ .

For each complex,  $\tau_f$  is very similar to that for the complex in the aqueous phase (ca. 500 ns) but  $\tau_s$  is significantly longer (>2000 ns). Furthermore,  $\tau_s/\tau_f$  increases as the ratio  $[DNA]/[Ru]$  increases.<sup>23</sup> For example, when  $[DNA]/[Ru]$  is ca. 10,  $\tau_f$  comprises 80% of the total decay, but when  $[DNA]/[Ru]$  is ca. 100,  $\tau_f$  comprises only 25% of the total decay. In other words, the contribution from the territorially bound relative to the interfacially bound complex decreases as the

amount of DNA increases. These results allow confirmation of the conclusion that the DNA-bound complex is responsible for the longer lived component.

$$I(t) = A_f \exp(-t/\tau_f) + A_s \exp(-t/\tau_s) \quad (4)$$

### The Nature of the Binding of Metal Complexes to DNA

Are the two complexes  $Ru(phen)_3^{2+}$  and  $Ru(DIP)_3^{2+}$  surface bound (possibly in rapid equilibrium with the territorial site) and/or intercalatively bound to the DNA interfacial region? An important observation relevant to this question was found in the discovery that *the photophysical parameters report a difference in the binding modes and efficiencies of enantiomeric pairs of the two complexes*. In particular, the  $\Delta$ - $Ru(phen)_3^{2+}$  and the  $\Delta$ - $Ru(DIP)_3^{2+}$  enantiomers (Figure 1) are more strongly bound to the interfacial region than the corresponding  $\Lambda$  enantiomers.<sup>22</sup> The enantiomeric selectivity for binding to B-DNA is modest in the case of the  $\Delta, \Lambda$ - $Ru(phen)_3^{2+}$  pair, but nearly *quantitative* in the case of the  $\Delta, \Lambda$ - $Ru(DIP)_3^{2+}$  pair.

From these photophysical data, together with more traditional, nonphotochemical measures,<sup>24</sup> it was concluded that the  $\Delta$ - $Ru(phen)_3^{2+}$  complex was surface or intercalatively bound to the DNA and the  $\Lambda$ - $Ru(phen)_3^{2+}$  complex was surface or territorially bound. For example, the retention of polarization was greater for the  $\Delta$ - $Ru(phen)_3^{2+}$  isomer than for the  $\Lambda$ - $Ru(phen)_3^{2+}$  isomer. It was also concluded that the  $\Delta$ - $Ru(DIP)_3^{2+}$  complex was intercalatively bound and the  $\Lambda$ - $Ru(DIP)_3^{2+}$  complex was surface bound. Indeed, the absolute degree of polarization for the  $\Delta$ - $Ru(DIP)_3^{2+}$  complex is nearly as great as the limiting value for complete rigidity, i.e.,  $\Delta$ - $Ru(DIP)_3^{2+}$  is firmly anchored to the DNA framework, as confirmed by molecular models and computer modeling.

Simple polarization measurements reveal the mode of binding and the enantiomeric selectivity for  $\Delta$ - $Ru(phen)_3^{2+}$  over  $\Lambda$ - $Ru(phen)_3^{2+}$ , because the former shows a substantial polarization (interfacially bound), whereas the latter shows no polarization (territorially bound or engaging in rapid equilibration with surface binding). Furthermore, in the presence of B-DNA,  $Co(phen)_3^{3+}$  "quenches" the polarization of  $^*rac$ - $Ru(phen)_3^{2+}$ , whereas with  $Fe(CN)_4^{4-}$  as "quencher", the polarization is "enhanced". These results demonstrate that the  $rac$ - $Ru(phen)_3^{2+}$  is bound to the DNA Stern layer and not territorially bound. Furthermore, the consistently larger polarization for  $\Delta$ - $Ru(phen)_3^{2+}$  relative to  $\Lambda$ - $Ru(phen)_3^{2+}$  is consistent with a tighter binding, i.e., intercalation rather than surface binding.

The conclusions based on the rather simple photophysical parameters allow the construction of an intuitively pleasing pattern for binding of a family of metal complexes to B-DNA (Figure 5): the most hydrophilic complex,  $Ru(bpy)_3^{2+}$ , likes the water phase and binds territorially; the more hydrophobic complex,  $Ru(phen)_3^{2+}$ , is attracted to the DNA interface by a combination of electrostatic and hydrophobic interactions in the minor groove, but does not possess a ligand size that is very effective for intercalation (however, modest enantiomeric discrimination does exist and the  $\Delta$ - $Ru$ -

(22) (a) Kumar, C. V.; Barton, J. K.; Turro, N. J. *J. Am. Chem. Soc.* 1985, 107, 5518. (b) Barton, J. K.; Goldberg, J. M.; Kumar, C. V.; Turro, N. J. *J. Am. Chem. Soc.* 1986, 108, 2081. (c) Barton, J. K.; Kumar, C. V.; Turro, N. J. *J. Am. Chem. Soc.* 1986, 108, 6391. (d) Pyle, A. M.; Rehmann, J. P.; Meshoyrer, R.; Kumar, C. V.; Turro, N. J.; Barton, J. K. *J. Am. Chem. Soc.* 1989, 111, 3051.

(23) Kirsch-DeMesmaeker, A.; Orellana, G.; Barton, J. K.; Turro, N. J. *Photochem. Photobiol.* 1990, 52, 461–472.

(24) (a) Barton, J. K.; Dannenberg, J. J.; Raphael, A. L. *J. Am. Chem. Soc.* 1982, 104, 4967. (b) Rehmann, J. P.; Barton, J. K. *Biochemistry* 1990, 29, 1701–1709, 1710–1717.



**Figure 5.** Computer-generated model of the binding of  $\text{Ru}(\text{bpy})_3^{2+}$  (green, in the Gouy–Chapman layer),  $\Delta\text{-Ru}(\text{phen})_3^{2+}$  (yellow, intercalatively bound in the major groove), and  $\Lambda\text{-Ru}(\text{phen})_3^{2+}$  (red, surface bound in the minor groove). The sugar phosphate backbone is in purple and the base pairs are in blue.

$(\text{phen})_3^{2+}$  form appears to bind intercalatively). The very hydrophobic complex,  $\text{Ru}(\text{DIP})_3^{2+}$ , is squeezed out of the water onto the DNA interface and possesses an extended aromatic ligand structure that allows intercalation into the base pairs of the major groove.

Binding by intercalation into the right-handed helix favors the  $\Delta$  isomer for both phen and DIP complexes, because of the reduced steric constraints between the ligands and the phosphate backbone. For the intercalative mode, the  $\Delta$  complex may be viewed as intercalating in the right-handed helix with a symmetry that matches the symmetry of the DNA surface. For the surface-bound mode, in contrast, a complementary symmetry is required. It is the  $\Lambda$  isomer that is favored for binding against the surface of the right-handed helix. This allows the nonintercalated ligands to minimize their steric interactions with the phosphate backbone. The results clearly demonstrate that the selectivity of molecular recognition of the sites on DNA for the substrate metal complexes is a sensitive feature

of the binding mode, with sensitivity for the size, shape, and chirality increasing as the mode goes from territorial to surface to intercalative binding.

#### Binding Mode Dependent Rates of Photoinduced Electron Transfer between Metal Complexes Bound to DNA. Site and Enantiomeric Selectivity

How does the value of the rate constant for photoinduced electron transfer,  $k_{\text{et}}$ , vary as a function of the structure of the  $\text{RuL}_3/\text{DNA}$  associate? In principle, territorially bound, surface-bound, and intercalatively bound excited donors could be compared for a variety of quenchers, and the values of enantiomeric  $\text{RuL}_3/\text{DNA}$  surface and intercalative associates could be determined. Toward this end, the photoinduced electron transfer between  $\text{Ru}(\text{phen})_3^{2+}$  complexes and  $\text{CoL}_3^{3+}$  quenchers was selected for model studies.<sup>20</sup>

From both photophysical and classical parameters for binding,<sup>17</sup>  $\text{Ru}(\text{phen})_3^{2+}$  and  $\text{Co}(\text{phen})_3^{3+}$  complexes bind



**Table II.**  
**Rate Constants for Photoinduced Electron Transfer from the Donors  $\Delta$ -Ru(phen) $_3^{2+}$  and  $\Lambda$ -Ru(phen) $_3^{2+}$  to *rac*-Co(phen) $_3^{3+}$  and *rac*-Co(bpy) $_3^{3+}$  in the Presence of DNA<sup>a</sup>**

donor	acceptors					
	Co(phen) $_3^{2+}$			Co(bpy) $_3^{2+}$		
	$k_q^s, M^{-1} s^{-1}$	$k_q^i, M^{-1} s^{-1}$	$k_q^c, M^{-1} s^{-1}$	$k_q^s, M^{-1} s^{-1}$	$k_q^i, M^{-1} s^{-1}$	$k_q^c, M^{-1} s^{-1}$
$\Delta$ -Ru(phen) $_3^{2+}$	$1.7 \times 10^{10}$	$0.9 \times 10^{10}$	$0.14 \times 10^{10}$	$2.4 \times 10^{10}$	$1.2 \times 10^{10}$	$0.20 \times 10^{10}$
$\Lambda$ -Ru(phen) $_3^{2+}$	$3.9 \times 10^{10}$	$1.6 \times 10^{10}$	$0.14 \times 10^{10}$	$4.7 \times 10^{10}$	$1.7 \times 10^{10}$	$0.20 \times 10^{10}$

<sup>a</sup>The rate constants  $k_q^s$ ,  $k_q^i$ , and  $k_q^c$  stand for the rates of electron transfer for the surface-bound, intercalated, and free donor (control) in solution, respectively. The estimated error in the rate constants is no more than 20%. The control data employed *rac*-Ru(phen) $_3^{2+}$  in the absence of DNA.

both by a surface (s) and an intercalated (i) mode to DNA. Thus, photoinduced electron transfer may be studied between a surface (\*s-Ru(phen) $_3^{2+}$ ) or intercalated (\*i-Ru(phen) $_3^{2+}$ ) donor and quenchers that are bound to the DNA in different modes.<sup>21</sup> Recall that the time-resolved emission of the \*Ru(phen) $_3^{2+}$  bound to DNA shows two decay components, the shorter of which (ca. 500 ns) is assigned to the surface-bound complex and the longer of which (ca. 2000 ns) is assigned to the intercalated component. The rate constants for quenching of each component were evaluated from Stern-Volmer quenching (eq 5) by *rac*-Co(phen) $_3^{3+}$ . In eq 5,  $\tau$  is the lifetime of the shorter (or longer) lived component at a concentration of quencher equal to [Q];  $\tau_0$  is the lifetime of the component in the absence of quencher; and  $k_{et}$  is the rate constant for electron-transfer quenching ( $k_{et}^i$  and  $k_{et}^s$ , for the intercalated and surface-bound donors, respectively) for each component.

$$\tau_0/\tau = 1 + k_{et}\tau_0[Q] \quad (5)$$

If the assumption that both components of the emission derive from donors that are surface-bound or intercalatively bound to the DNA is true, then it is expected that *both* components will show enantiomeric selectivity toward electron transfer. The results<sup>25</sup> given in Table II support the assumptions and provide insight to the nature of the electron-transfer mechanism. First, it is seen that there is a clear *enantiomeric selectivity* in the quenching of  $\Delta$ -Ru(phen) $_3^{2+}$  and  $\Lambda$ -Ru(phen) $_3^{2+}$  by *rac*-Co(phen) $_3^{3+}$ . The value of  $k_{et}$  for the surface-bound  $\Lambda$ -Ru(phen) $_3^{2+}$  complex is nearly twice as large as that for the  $\Delta$ -Ru(phen) $_3^{2+}$  complex. In addition, the value of  $k_{et}$  for the *surface-bound* component for either enantiomer is about 2 times greater than the value of the *intercalatively bound* component. Finally, the values of  $k_{et}$  (ca.  $1\text{--}4 \times 10^{10} M^{-1} s^{-1}$ , in the same units as those for *intermolecular* electron transfer) are over an order of magnitude larger than the values obtained for the aqueous phase ( $k_{et} = 1.4 \times 10^9 M^{-1} s^{-1}$ , respec-

tively) in the absence of DNA. In parallel experiments, although the same trends are followed, the more hydrophilic and presumably more mobile Co(bpy) $_3^{3+}$  as a quencher yields somewhat higher quenching constants.

These results point clearly to a greater electron-transfer efficiency when the donor is surface bound relative to the intercalatively bound donor ( $k_{et}^s > k_{et}^i$ ). This suggests that the rate of electron transfer on the DNA is sensitive to the rate of mobility and transport of the donor-acceptor pair along the DNA helix. Next, the faster quenching of the more loosely bound enantiomer ( $k_{et}^\Lambda > k_{et}^\Delta$ ) suggests that, for either binding mode, the rate of electron transfer is sensitive to enantiomeric structure because of differing rates of transport of each enantiomer along the DNA helix (the  $\Delta$  form is generally a better binder than the  $\Lambda$  form of the complexes). These results were obtained for relatively "dilute" concentrations of the donor complex along the DNA helix (Ru/DNA < 0.01), conditions such that all of the metal complexes are bound to the DNA. At higher concentrations of the donor along the helix, the observed rate constants are governed by large local concentrations of donors and acceptors to the DNA and hence by the magnitude of the binding constants.

The results clearly demonstrate the role of binding to a restricted reaction space in the efficiency and rate of electron-transfer process. A number of important issues remain to be pursued. For example, on the one hand, do the rules for electron transfer that have been theoretically<sup>22</sup> and experimentally<sup>23</sup> examined over the past several decades obtain for electron transfer between species bound to restricted spaces? On the other hand, does the restricted space play an active "electronic" role, or is it only a template to direct a traffic pattern to transport reactants? Experiments to examine these questions are currently under active investigation.

*We acknowledge with great pleasure the contributions of our co-workers whose experimental and intellectual contributions have made these investigations so stimulating and educational to the senior authors: Dr. Challa V. Kumar and Dr. Gabriella Caminati. We also thank the following agencies for their generous support of this research: the National Science Foundation, the Air Force Office of Scientific Research, and the National Institutes of Health.*

(25) (a) Barton, J. K.; Kumar, C. V.; Turro, N. J. *J. Am. Chem. Soc.* **1986**, *108*, 6391. (b) Purugganan, M. D.; Kumar, C. V.; Turro, N. J.; Barton, J. K. *Science* **1988**, *241*, 1645.

(26) (a) Marcus, R. *Annu. Rev. Phys. Chem.* **1964**, *15*, 155; (b) *J. Phys. Chem.* **1968**, *72*, 891. (c) Marcus, R.; Sutin, N. *Biochim. Biophys. Acta* **1985**, *811*, 265.

(27) Closs, G. L.; Calcaterra, L. T.; Green, N. J.; Renfield, K. W.; Miller, J. R. *J. Phys. Chem.* **1986**, *90*, 3673.